Fluctuating Atlantic inflows modulate Arctic atlantification

Igor V. Polyakov[1*], Randi B. Ingvaldsen[2], Andrey V. Pnyushkov[3], Uma S. Bhatt[4], Jennifer A. Francis[5], Markus Janout[6], Ronald Kwok[7], Øystein Skagseth[2,8]

1 International Arctic Research Center and College of Natural Science and Mathematics, University of Alaska Fairbanks; N130 Koyukuk Drive, Fairbanks, AK, 99775, USA

2 Institute of Marine Research; Nordnesgaten 50, 5005, Bergen, Norway.

3 International Arctic Research Center, University of Alaska Fairbanks; 930 Koyukuk Drive, Fairbanks, AK, 99775, USA

4 Geophysical Institute and College of Natural Science and Mathematics, University of Alaska Fairbanks; 2156 Koyukuk Drive, Fairbanks, AK, 99775, USA,

5 Woodwell Climate Research Center; 149 Woods Hole Rd., Falmouth MA 02540, USA

6 Alfred-Wegener-Institute, Helmholtz Centre for Polar and Marine Research; Am Handelshafen 12, D-27570 Bremerhaven, Germany

7 Polar Science Center, Applied Physics Lab, University of Washington; 1013 NE 40th Street, Seattle, WA 98105, USA

8 Bjerknes Centre for Climate Research; Bergen, Norway

Type of the manuscript: Original Research. Figures/tables: 5/0. Length: 3224 words.

*Corresponding author: Igor V. Polyakov, 907-474-2686, ivpolyakov@alaska.edu

Abstract

Enhanced warm, salty sub-Arctic inflows drive high-latitude atlantification, weakening oceanic stratification, amplifying heat fluxes, and reducing sea ice. Here we show that the atmospheric Arctic Dipole (AD) associated with anticyclonic winds over North America and cyclonic winds over Eurasia modulates inflows from the North Atlantic across the Nordic Seas. The alternating AD phases create a "switchgear mechanism." In 2007–2021, switchgear weakened northward inflows and enhanced sea-ice export across Fram Strait, and increased inflows throughout the Barents Sea. By favoring stronger Arctic Ocean circulation, transferring freshwater into the Amerasian Basin, boosting stratification, and lowering oceanic heat fluxes there after 2007, AD+ contributed to slowing sea-ice loss. A transition to a new AD– phase may accelerate the Arctic sea-ice decline, furthering Arctic climate system's changes.

One-Sentence Summary: Shifts in a large-scale atmospheric pattern have influenced Arctic Ocean currents with profound consequences for the Arctic climate system.

Introduction

The Arctic region is rightfully called a frontier for global climate change. Linked to atmospheric circulation, radiative forcing, and a host of climate feedback mechanisms, Arctic surface air temperatures are rising at least three times faster than global-average air temperatures (*1*). The Arctic Ocean is warming faster than the global ocean (*2*). Sea-ice decline is a true indicator of climate change, affecting all aspects of life in the northern high-latitude regions (*1*). One of the reasons for sea-ice loss is the warming Arctic Ocean caused in part by anomalous inflows from the North Atlantic and North Pacific (e.g., *3-5*). System-wide changes in Arctic basins caused by anomalous inflows from the Nordic Seas are referred to as atlantification (e.g., *5-7*). One of many manifestations of atlantification in the Eurasian Basin of the Arctic Ocean is decreased upper-ocean stratification and enhanced heat release from the warm intermediate (150-800 m depth) Atlantic Water layer, resulting in accelerated loss of sea ice (*5, 8, 9*). However, these changes are complex, and their driving forces and interactions with the Arctic atmosphere–ice–ocean system are not well understood. This study identifies important mechanisms steering high-latitude atlantification, informing a broad and comprehensive understanding of system function.

Sea ice changes

While the end-of-summer ice extent and thickness are declining, our results indicate that the rate of decline slowed after 2007 compared with 1992–2006 (**Figs. 1a,b**). Over the satellite record, the trend in summer ice extent during 2007–2021 ($-0.07\pm0.18\times10^6$ km^2 per decade) is weak and not statistically significant in contrast to the much larger negative trends in 1979–2021 ($-0.79\pm0.13\times10^6$ km^2 per decade) and 1992–2006 ($-0.99\pm0.51\times10^6$ km^2 per decade). Thus, a more stable regime of Arctic sea ice appears to have begun in 2007. This transition

was abrupt, with 2007 setting a record for a single-year sea-ice-extent decrease of -1.6×10^6 km^2 (compare to 2012's second record-year drop of -1.0×10^6 km^2) (see for details *10*).

Similarly, the composite record of mean winter (February–March) ice thickness in the central Arctic, now close to ~2 m, has not changed significantly since 2007 (**Fig. 1a**), even though the multi-decadal decline has been significant. In addition, the mean thickness in fall (October–November) has remained above the 1m low established after the end of the summer of 2007. Between 2003 and 2007, the thinning was remarkable and occurred with the loss of a large fraction of thick multiyear sea ice (*11*). The overall thinning has slowed since 2007, when satellite-based records of ice thickness began (ICESat, ICESat-2, and CryoSat-2, 2003–2021). The Arctic is now dominated by the behavior of thinner seasonal ice, which now solely controls the variability of ice thickness in the central Arctic (*12, 13*).

Atmospheric changes

The atmosphere over the Arctic Ocean is dominated by high pressure (known as the Polar High) centered over the western Arctic (**Fig. 2a**), which generates a mean anticyclonic (clockwise) circulation. This drives predominant features of sea-ice drift and upper-ocean circulation known as the Beaufort Gyre in the Amerasian Basin as well as the Transpolar Drift flowing from the Siberian shelf towards the Canadian Archipelago and Fram Strait (**Fig. 1g**).

The primary mode of variability of the pan-Arctic sea-level pressure is known as the Arctic Oscillation, and the related wind pattern accounts for the observed climatological features of the atmospheric circulation. Beginning in 2007, however, the secondary Arctic Dipole (AD) pattern, featuring higher sea-level pressure over the Beaufort Gyre and the Canadian Archipelago along with lower sea-level pressure over the Siberian Arctic, became dominant (**Fig. 2c**; see also *16-18*), whereas the Arctic Oscillation remained close to neutral

(**Fig. S4**). This shift is evident in the higher spatial correlation between the mean 2007−2021 sea-level pressure and AD (R=0.59), compared to that with Arctic Oscillation (R=0.47).

The AD index, a characteristic of the wind cyclonicity in the central and Siberian Arctic (*16*), varies between positive (AD+) and negative (AD–) over ~15-year regimes (see wavelets in **Figs. S2, S3**). During 1992–2006, both the AD and Arctic Oscillation indices were slightly negative (**Fig. S4d,e**), while during 2007–2021 the AD index became increasingly positive (**Fig. S4e**).

The AD+ drives an enhanced anticyclonic Beaufort Gyre and Transpolar Drift (*19*), **Fig. 2**. Distinct from the Arctic Oscillation (*20, 21*), the across-pole AD pattern results in increased heat advection into the Arctic, especially along the Siberian shores (**Fig. 2b),** and contributes to higher surface-air temperatures (**Fig. S3**). The AD was a major driver of the second record-low sea-ice extent in summer 2007 during the satellite record (*22*). The Fram Strait sea-ice export is correlated with the AD index during 1979–2014 (significant R=0.45, (*19*), see **Fig. 2d**), with a stronger link to the AD than to the Arctic Oscillation (*23*).

Most important for the present study, the alternating AD phases were pivotal for a switchgear mechanism modulating the relative strength of the Fram Strait and Barents Sea branches transporting Atlantic Water into the Arctic Ocean. For example, the anomalous atmospheric forcing during the AD+ in 2007–2021 was favorable for reduced flows into the Arctic through the Fram Strait along with enhanced inflows through the Barents Sea Opening (**Fig. 2b,e,f**). The Arctic Oscillation pattern contributes to large-scale cyclonicity in Arctic atmosphere, ocean, and ice circulation (e.g., *24*) but not the finer details suggested by the switchgear mechanism discussed here (**Fig. S4**). The AD-driven forcing is best developed in spring and summer (**Figs. S2, S5**), but can affect air temperatures, surface energy fluxes,

storm tracks, sea-ice drift and exports, and upper-ocean circulation in all seasons (e.g., **Fig. S3**).

Changes in the Arctic Ocean

Switchgear between Fram Strait inflow and Barents Sea throughflow

Water exchanges between the Nordic Seas and the Arctic Ocean are critically important for the state of the Arctic climate system. ORAS5 reanalysis data (see Supplementary Materials for details) suggest that these exchanges in the upper 50 m were amplified across the northern Barents Sea Opening and in the northern and central Barents Sea while being reduced across the Fram Strait in the past 15 years (**Fig. 3**), with similar patterns but weaker anomalies in the 50–200 m layer (**Fig. S6**). Time series of currents across the Barents Sea Opening and Fram Strait clearly show this alternating pattern, with 5% increased annual mean currents in the Barents Sea Opening and 15% decrease in Fram Strait (**Fig. 3c,d**). Summer and fall ORAS5 transports were the most significant contributors to anomalous Barents Sea Opening inflows (15% increase), while spring and summer processes dominated Atlantic Water inflows through Fram Strait (28% decrease in current speed) (**Fig. S7**). At the 95% confidence level, each of the aforementioned estimates of anomalous transports is statistically significant. In comparison to the Barents Sea Opening, changes in the upper 50m water volume transports were ~2.2 times stronger in the Fram Strait. As a result, changes in transports through these gateways do not countervail, and the importance of other gateways in establishing the Arctic Ocean's water balance cannot be overstated. On weekly-to-monthly time scales, increased eastward flow in the northern Barents Sea and weakened inflow across the Fram Strait are associated with a northward shift in atmospheric cyclones over the Barents Sea (*25*).

Amplified Barents Sea Opening inflows in 2007–2021 resulted in increased transports across the Franz Joseph Land–Novaya Zemlya pass by 23%, thus providing an enhanced

inflow from the Barents Sea into the Arctic Ocean (**Figs. 3g, S8**). These changes were crucial for the new state of the eastern Arctic Ocean brought on by atlantification (*5*). Tracer experiments showed a doubled probability that water parcels in the upper 50m crossed the Barents Sea in 2007–2021 compared with 1992–2006, in contrast with Fram Strait, where the number of tracers decreased over the same time by a factor of four (**Fig. 4d,e**). Stronger impacts of the local winds on the Barents Sea compared with Fram Strait inflows are consistent with stronger topographic steering and more complex flow in the Fram Strait (*26, 27*).

These findings are strongly supported by both *in situ* and satellite observations. For example, mooring and reanalysis records are positively correlated and show consistent increasing (decreasing) trends of currents across the Barents Sea Opening (Fram Strait) over the last 15 years (**Fig. S9**). A modest correlation R=0.34 between the Barents Sea Opening mooring and reanalysis time series is likely because moorings do not cover the northern regions where the reanalysis shows the greatest increase in flow. Moreover, anomalies in the satellite-based sea-surface height provide further confirmation for the switchgear mechanism modulating the inflows through the Barents Sea and Fram Strait during the current AD+ (**Fig. 4g**). Geostrophic currents forced by the anomalous 2007–2021 sea-surface height were amplified in the northern Barents Sea Opening and in the central Barents Sea showing little difference in the southern Barents Sea Opening. However, the sea-surface height indicates an anomalous flow from the Lofoten Basin to the Barents Sea in 2007–2020 (**Fig. 4g**). The possibility of the Lofoten Basin feeding the Barents Sea has been suggested by (*28*), attributed to the vigorous eddy activity in the Lofoten Basin (*29, 30*), and is further linked to the atmospheric wind forcing (*31*). In contrast to the Barents Sea Opening, the geostrophic flow across Fram Strait weakened (**Fig. 4g**).

Imprints of alternating AD patterns on the Arctic Ocean circulation

The Arctic basins responded to the AD+ atmospheric regime in 2007–2021 with basin-wide changes in the upper Arctic Ocean circulation associated with an amplified Beaufort Gyre, stronger boundary currents along the Siberian slope, and a shifted Transpolar Drift from the Amerasian Basin towards the Lomonosov Ridge (**Fig. 3b, 4a,b**).

Since 2007, a smaller but more intense Arctic high, associated wind-driven circulation, and convergence of the upper Beaufort Gyre have resulted in enhanced freshening and thickening of the surface fresh layer in the Amerasian Basin (e.g., *24, 32*). The Beaufort Gyre mooring record provides confirmation of these findings (**Fig. 5a,b**). This evidence is further supported by observed sea-ice melt, redirected Siberian riverine waters into the Beaufort Gyre, increasing inflow of relatively fresh Pacific Water through Bering Strait, and strengthened stratification between the Amerasian Basin's surface and deep layers (e.g., *24, 32, 33, 34*). At the same time, reanalysis and mooring observations showed contrasting changes in the Eurasian Basin, with increased salinification and weakened stratification in the halocline, along with amplified upward heat fluxes (*5, 35*), **Fig. 5c,d**.

Our tracer experiments support these findings (**Figs. 4a-c, S11**). For example, the 2007–2021 cyclonic atmospheric forcing widely dispersed transports of freshwater from the Siberian shelves (where the Transpolar Drift originates) and drove a substantial portion (17% of all trajectories) of the Siberian freshwater into the Beaufort Gyre. In contrast, during the anticyclonic 1992–2006 AD– phase, not a single water parcel ended up trapped in the Beaufort Gyre, and instead left the central Arctic through the straits of the Canadian Archipelago. Changes in the spatial distributions of meteoric water (i.e., precipitation including water from lakes and rivers) provide confirmation of the diversion of freshwater from the Eurasian Basin to the Amerasian Basin, with meteoric water content decreasing in

177 the Eurasian Basin and increasing in the Amerasian Basin, consistent with (*36, 37*). These
178 changes in meteoric water content are accompanied by a general increase in net sea-ice
179 meltwater (**Fig. S12**).

180 In the Eurasian Basin, the local effects of alternating AD patterns and the remote effects of
181 atlanticification owing to changing influxes across Fram Strait and Barents Sea are
182 interconnected in an ice/ocean-heat feedback mechanism. Weakened stratification and
183 increased oceanic heat fluxes associated with atlantification drive sea-ice melt, which is
184 amplified by increased oceanic heat fluxes through increased convective entrainment in
185 winter (*5, 9*). A stronger coupling between atmosphere, ice, and ocean in the eastern Arctic in
186 the recent decade and intensified upper-ocean currents play critical roles in developing this
187 feedback (*38*), **Fig. 3b**.

188 **Changes in the Nordic Seas**

189 Anomalous anticyclonic winds over the Nordic Seas, as evident during the AD+ in 2007–2021
190 (**Fig. 2b**), weakened the poleward Atlantic Water flow from south of the sub-polar gyre and
191 through the Nordic Seas (*27, 39*). Attributed to a weak reinforcement of the sub-polar gyre
192 (**Fig. S13**), altering the properties of the inflowing Atlantic Water (*40*), the Atlantic Water
193 inflow from the northern North Atlantic became colder and fresher in the late 2000s (*41*), **Figs.**
194 **5q,r**. The Atlantic Water temperatures and salinities in the Nordic Seas and the Barents Sea
195 Opening responded to this change by peaking in the late 2000s (**Figs. 5m-p**).

196 Consistent with these changes, the salinity trends in the Nordic Seas after 2006/2007 are
197 negative and similar in magnitude from the North Atlantic up to the Barents Sea Opening (**Fig.**
198 **5r,p,n,j,i**). Atmospheric circulation over the Nordic Seas associated with the AD+ in 2007–
199 2021 (**Fig. 2b**) weakened the northward Norwegian Atlantic Current (**Fig. 3b**, *42*), which is
200 consistent with a negative trend of –3cm/s per decade shown by the mooring record from

Svinøy section, the gateway for the Atlantic Water into the Nordic Seas (**Fig. S9**). Despite these changes in the Nordic Seas, the salinity in the eastern Eurasian Basin halocline and Atlantic Water increased (**Fig. 5d**), driven by salinification in the upstream northern Barents Sea due to lack of meltwater input from seasonal ice melt (*43*).

The cooling trend in 2007–2021 is reduced along-stream the Atlantic Water from the northern North Atlantic into the Barents Sea and Fram Strait (–0.55°C in the North Atlantic/Rockall, –0.36°C at Svinøy, and insignificant farther north, **Fig. 5**). These changes in the Nordic Seas are supported by the reduced oceanic heat loss over the last decades (*44*). Thus, the traditional paradigm of Atlantic Water variability associated with either cold and fresh or warm and saline Atlantic Water has changed (**Fig. 5e-n**). Moreover, our analysis confirms a northward amplification of oceanic warming (*7*), with the origin in the Nordic Seas, making this a source region of atlantification and Arctic amplification.

We note that the observed temperature and salinity trends are also consistent with the switchgear-driven stronger flow through the Barents Sea Opening compared with Fram Strait flow after 2006/2007, with temperatures at the Barents Sea Opening and northeastern Barents Sea showing little or no decrease (**Fig. 5g,k**), while the Frams Strait temperatures fell rapidly (**Fig. 5e,i)**. Since the mid-2000s, the along-track heat loss of the Fram Strait inflow has increased (*45*), while the heat loss of the Barents Sea throughflow has decreased or remained stable (*45, 46*), thereby implying a stronger warming of the Atlantic Water entering the Arctic from the Barents Sea as compared to Fram Strait. Thus, a combination of the switchgear and regional changes in heat loss make the Barents Sea a key contributor to the Arctic Ocean atlantification.

Discussion

This research identifies the mechanisms driving atlantification and paints a broad and comprehensive picture of changes in the northern high-latitude climate system. Switchgear is one of these mechanisms resulting from alternating AD atmospheric regimes. We discovered increased Atlantic Water inflows throughout the Barents Sea and reduced inflow across Fram Strait as well as a stronger warming of the Barents Sea as compared to Fram Strait during 2007–2021. This regime was also associated with the amplified Beaufort Gyre, stronger boundary currents at the Siberian slope, and a shifted Transpolar Drift from the Amerasian Basin towards the Lomonosov Ridge.

One of the most striking changes associated with AD variability is the 2007-2021 hiatus of Arctic summer sea-ice loss, which, we argue, is a response to enhanced redistribution of freshwater into the Amerasian Basin caused by anomalous winds and increased stratification that suppress oceanic heat fluxes. This process is regionally limited to the Amerasian Basin, where the sea-ice area has actually increased since 2007 (**Fig. 1d,e**). Thus, while variations in atmospheric forcing may affect the ice-loss slowdown since 2007 (*47*), the shutting down of oceanic heat fluxes by increasing Amerasian Basin stratification (**Fig. 1b**, insert) may help drive the ice-loss hiatus. To validate this hypothesis, we used the winter survival of the near-surface temperature maximum created by the summer trapping of solar radiation below the surface mixed layer (10–30 m depth) (*48*). Using an extensive 2007–2020 archive of Ice-Tethered Profiler observations, we found that 65% of vertical temperature profiles showed the presence of the near-surface temperature maximum (and therefore negligible upper Amerasian Basin ventilation) during October–March (**Fig. S14**; see Methods for details) – a convincing argument that enhanced sea-ice winter growth owing to reduced ocean heat fluxes contributed to the observed 2007–2021 ice-loss hiatus. Sea-ice dynamics should not be disregarded, though. For example, despite increased ice-area export (**Fig. 2d**), decreased ice thickness in Fram Strait (*10*) may cause a decline in ice volume export, offsetting the decline

249 in net ice production in high-latitude regions (e.g., *49*). In contrast to the Amerasian Basin,
250 ventilation of the upper Eurasian Basin in the 2010s is well documented (e.g., *5, 9, 38*), and
251 sea-ice loss in this basin continued through the 2010s (**Fig. 1d,e**).

252 There are numerous ongoing and potential ecological consequences of the observed
253 physical changes. For example, the summer-integrated Normalized Difference Vegetation
254 Index (TI-NDVI), a remotely sensed proxy for Arctic vegetation productivity, shows
255 remarkably different behavior during AD+ and AD–. The TI-NDVI trends at all longitudes
256 were primarily positive in 1992–2006, suggesting the vegetation gained biomass and
257 photosynthetic productivity increased; the vegetation was 'greening' (**Fig. 1c,f**). In 2007–
258 2021, negative trends dominated the area between 210°E-300˚E (corresponding to the
259 Amerasian Basin sector where sea ice increased during 2007–2021), suggesting the
260 vegetation lost biomass and was possibly less vigorous; often called 'browning' (**Fig.**
261 **1d,f**). Thus, sea ice variability can influence Arctic vegetation productivity on numerous time
262 scales, consistent with a correlation between the TI-NDVI and spring sea-ice variations (*50*).
263 Furthermore, the import of sub-Arctic waters has profound impacts on Arctic marine life
264 (*51*), and both the Fram Strait and the Barents Sea Opening branches are potential pathways
265 of subarctic-boreal organisms into the eastern Eurasian Basin (*52*). Our results suggest that
266 organisms drifting in the upper 50 m of the Fram Strait branch had a fundamentally different
267 fate if entering during AD– as compared to AD+ (**Fig. 4d-e**). During AD– most organisms
268 entered the western Eurasian Basin via the Transpolar Drift, while during AD+ they were
269 kept at the shelf break and transported into the eastern Eurasian Basin. In addition, during
270 AD+, more organisms entered the eastern Eurasian Basin from the Barents Sea (**Fig. 4e**).
271 Increased influence of the Barents Sea may cause the eastern Eurasian Basin to be more
272 productive and provide more suitable living conditions for subarctic-boreal species than its

273 western part (*53*), which is consistent with recent observations (*52*). Improved knowledge of
274 asymmetric conditions in the pelagic ecosystems of the western and eastern Eurasian Basin is
275 imperative to properly understand and manage the central Arctic Ocean fisheries agreement
276 established in 2021.

277 Finally, we note that recent atmospheric changes as indicated by a shifting AD phase have
278 been important drivers of the regional patterns of sea ice and oceanic responses. There are,
279 however, indications that the Arctic system may be entering another new regime (see
280 wavelets in **Figs. S3, S7, S8**), with potential consequences for the state of the physical,
281 chemical, and biological components. The transition may be abrupt, similar to the rapid
282 changes in 2007. The trajectory of the Arctic climate system into the future is further
283 complicated by the existence of large-amplitude, multidecadal variability (**Fig. S15)**. Thus,
284 accurate future projections require a comprehensive understanding of complex air-ice-ocean
285 interactions and associated feedbacks on broad spatiotemporal scales through advancement of
286 the observing system and modeling capabilities.

References and Notes

1. IPCC, *Climate Change 2022: Impacts, Adaptation, and Vulnerability.* Contribution of Working Group II to the Sixth Assessment Report of the Intergovernmental Panel on Climate Change [H.-O. Pörtner, D.C. Roberts, M. Tignor, E.S. Poloczanska, K. Mintenbeck, A. Alegría, M. Craig, S. Langsdorf, S. Löschke, V. Möller, A. Okem, B. Rama (eds.)]. Cambridge University Press, Cambridge, UK and New York, NY, USA., 3056 pp. (2022). doi:3010.1017/9781009325844.
2. Q. Shu, Q. Wang, M. Arthun, S. Wang, Z. Song, M. Zhang, and F. Qiang, Arctic Ocean Amplification in a warming climate in CMIP6 models. Sci. Adv. 8(30), , DOI: 10.1126/sciadv.abn9755.
3. R. A. Woodgate, T. Weingartner, R. Lindsay, The 2007 Bering Strait oceanic heat flux and anomalous Arctic sea-ice retreat. *Geophys. Res. Lett.***37**, L01602 (2010).
4. K. Shimada, T. Kamoshida, M. Itoh, S. Nishino, E. Carmack, F. McLaughlin, S. Zimmermann, A. Proshutinsky, Pacific Ocean inflow: Influence on catastrophic reduction of sea ice cover in the Arctic Ocean. *Geophys. Res. Lett.* **33**, L08605 (2006).
5. I. V. Polyakov, A. V. Pnyushkov, M. B. Alkire, I. M. Ashik, T. M. Baumann, E. C. Carmack, I. Goszczko, J. Guthrie, V. V. Ivanov, T. Kanzow, R. Krishfield, R. Kwok, A. Sundfjord, J. Morison, R. Rember, A. Yulin, Greater role for Atlantic inflows on sea-ice loss in the Eurasian Basin of the Arctic Ocean. *Science* **356**, 285-291 (2017).
6. I. V. Polyakov, M. B. Alkire, B. A. Bluhm, K. A. Brown, E. C. Carmack, M. Chierici, S. L. Danielson, I. Ellingsen, E. A. Ershova, K. Gardfeldt, R. B. Ingvaldsen, A. V. Pnyushkov, D. Slagstad, P. Wassmann, Borealization of the Arctic Ocean in Response to Anomalous Advection From Sub-Arctic Seas. *Front. Mar. Sci.* **7**, (2020).
7. R. B. Ingvaldsen, K. M. Assmann, R. Primicerio, M. Fossheim, I. V. Polyakov, A. V. Dolgov, Physical manifestations and ecological implications of Arctic Atlantification. *Nat. Rev. Earth Environ.* **2**, 874-889 (2021).
8. V. Ivanov, V. Alexeev, N. V. Koldunov, I. Repina, A. B. Sandø, L. H. Smedsrud, A. Smirnov, Arctic Ocean Heat Impact on Regional Ice Decay: A Suggested Positive Feedback. *J. Phys. Oceanogr.* **46**, 1437-1456 (2016).
9. I. V. Polyakov, T. P. Rippeth, I. Fer, M. B. Alkire, T. M. Baumann, E. C. Carmack, R. Ingvaldsen, V. V. Ivanov, M. Janout, S. Lind, L. Padman, A. V. Pnyushkov, R. Rember,

Weakening of Cold Halocline Layer Exposes Sea Ice to Oceanic Heat in the Eastern Arctic Ocean. *J. Clim.* **33**, 8107-8123 (2020).

10. H. Sumata, L. de Steur, D. V. Divine, M. A. Granskog, and S. Gerland, Regime shift in Arctic Ocean sea ice thickness. *Nature* **615**, 443–449 https://doi.org/10.1038/s41586-022-05686-x (2023).
11. R. Kwok, G. F. Cunningham, M. Wensnahan, I. Rigor, H. J. Zwally, D. Yi, Thinning and volume loss of the Arctic Ocean sea ice cover: 2003–2008. *J. Geophys. Res.* **114**, (2009).
12. R. Kwok, Arctic sea ice thickness, volume, and multiyear ice coverage: losses and coupled variability (1958–2018). *Environ. Res. Lett.* **13**, 105005 (2018).
13. S. Kacimi, R. Kwok, Arctic Snow Depth, Ice Thickness, and Volume From ICESat-2 and CryoSat-2: 2018–2021. *Geophys. Res. Lett.* **49**, e2021GL097448 (2022).
14. S. K. Gulev, P.W. Thorne, J. Ahn, F.J. Dentener, C.M. Domingues, S. Gerland, D. Gong, D.S. Kaufman, H.C. Nnamchi, J. Quaas, J.A. Rivera, S. Sathyendranath, S.L. Smith, B. Trewin, K. von Schuckmann, and R.S. Vose, , Changing State of the Climate System. In Climate Change 2021: The Physical Science Basis. Contribution of Working Group I to the Sixth Assessment Report of the Intergovernmental Panel on Climate Change [Masson-Delmotte, V., P. Zhai, A. Pirani, S.L. Connors, C. Péan, S. Berger, N. Caud, Y. Chen, L. Goldfarb, M.I. Gomis, M. Huang, K. Leitzell, E. Lonnoy, J.B.R. Matthews, T.K. Maycock, T. Waterfield, O. Yelekçi, R. Yu, and B. Zhou (eds.)]. Cambridge University Press, Cambridge, United Kingdom and New York, NY, USA, pp. 287–422, (2021). doi:10.1017/9781009157896.004.
15. Q. Wang, Shu, Q., S. Wang, A. Beszczynska-Moeller, S. Danilov, L. de Steur, T. W. N. Haine, M. Karcher, C. Lee, P. G. Myers, I. V. Polyakov, C. Provost, Ø. Skagseth, G. Spreen, and R. Woodgate, , A review of heat and freshwater fluxes through Arctic Ocean gateways: past changes, mechanisms and future projections. *Ocean-Land-Atmosphere Research.* Submitted, (2023).
16. B. Wu, J. Wang, J. E. Walsh, Dipole Anomaly in the Winter Arctic Atmosphere and Its Association with Sea Ice Motion. *J. Clim.* **19**, 210-225 (2006).
17. J. Zhang, R. Lindsay, M. Steele, A. Schweiger, What drove the dramatic retreat of arctic sea ice during summer 2007? *Geophys. Res. Lett.* **35**, L22701 (2008).
18. J. E. Overland, M. Wang, Large-scale atmospheric circulation changes are associated with the recent loss of Arctic sea ice. *TELLUS A* **62**, 1-9 (2010).

19. L. H. Smedsrud, M. H. Halvorsen, J. C. Stroeve, R. Zhang, K. Kloster, Fram Strait sea ice export variability and September Arctic sea ice extent over the last 80 years. *Cryosphere.* **11**, 65-79 (2017).
20. J. E. Overland, M. Wang, The third Arctic climate pattern: 1930s and early 2000s. *Geophys. Res. Lett.* **32**, L23808 (2005).
21. J. E. Overland, M. Wang, S. Salo, The recent Arctic warm period. *TELLUS A* **60**, 589-597 (2008).
22. J. Wang, J. Zhang, E. Watanabe, M. Ikeda, K. Mizobata, J. E. Walsh, X. Bai, B. Wu, Is the Dipole Anomaly a major driver to record lows in Arctic summer sea ice extent? *Geophys. Res. Lett.* **36**, L05706 (2009).
23. M. Tsukernik, C. Deser, M. Alexander, R. Tomas, Atmospheric forcing of Fram Strait sea ice export: a closer look. *Clim. Dyn.* **35**, 1349-1360 (2010).
24. J. Morison, R. Kwok, S. Dickinson, R. Andersen, C. Peralta-Ferriz, D. Morison, I. Rigor, S. Dewey, J. Guthrie, The Cyclonic Mode of Arctic Ocean Circulation. *J. Phys. Oceanogr.* **51**, 1053-1075 (2021).
25. V. S. Lien, F. B. Vikebø, Ø. Skagseth, One mechanism contributing to co-variability of the Atlantic inflow branches to the Arctic. *Nat. Commun.* **4**, 1488 (2013).
26. M. Muilwijk, L. H. Smedsrud, M. Ilicak, H. Drange, Atlantic water heat transport variability in the 20th century arctic ocean from a global ocean model and observations. *J. Geophys. Res.* **123**, 8159-8179 (2018).
27. M. Muilwijk, M. Ilicak, S. B. Cornish, S. Danilov, R. Gelderloos, R. Gerdes, V. Haid, T. W. N. Haine, H. L. Johnson, Y. Kostov, T. Kovács, C. Lique, J. M. Marson, P. G. Myers, J. Scott, L. H. Smedsrud, C. Talandier, Q. Wang, Arctic Ocean response to Greenland Sea wind anomalies in a suite of model simulations. *J. Geophys. Res.* **124**, 6286-6322 (2019).
28. S. Broomé, L. Chafik, J. Nilsson, A Satellite-Based Lagrangian Perspective on Atlantic Water Fractionation Between Arctic Gateways. *J. Geophys. Res.* **126**, e2021JC017248 (2021).
29. D. L. Volkov, T. V. Belonenko, V. R. Foux, Puzzling over the dynamics of the Lofoten Basin - a sub-Arctic hot spot of ocean variability. *Geophys. Res. Lett.* **40**, 738-743 (2013).

30. P. K. Jakobsen, M. H. Ribergaard, D. Quadfasel, T. Schmith, C. W. Hughes, Near-surface circulation in the northern North Atlantic as inferred from Lagrangian drifters: Variability from the mesoscale to interannual. *J. Geophys. Res.* **108**, (2003).
31. L. Chafik, J. Nilsson, Ø. Skagseth, P. Lundberg, On the flow of Atlantic water and temperature anomalies in the Nordic Seas toward the Arctic Ocean. *J. Geophys. Res.* **120**, 7897-7918 (2015).
32. A. Proshutinsky, R. Krishfield, J. M. Toole, M.-L. Timmermans, W. Williams, S. Zimmermann, M. Yamamoto-Kawai, T. W. K. Armitage, D. Dukhovskoy, E. Golubeva, G. E. Manucharyan, G. Platov, E. Watanabe, T. Kikuchi, S. Nishino, M. Itoh, S.-H. Kang, K.-H. Cho, K. Tateyama, J. Zhao, Analysis of the Beaufort Gyre Freshwater Content in 2003–2018. *J. Geophys. Res.* **124**, 9658-9689 (2019).
33. R. A. Woodgate, Increases in the Pacific inflow to the Arctic from 1990 to 2015, and insights into seasonal trends and driving mechanisms from year-round Bering Strait mooring data. *Prog. Oceanogr.* **160**, 124-154 (2018).
34. S. B. Hall, B. Subrahmanyam, M. Steele, The role of the Russian Shelf in seasonal and interannual variability of Arctic sea surface salinity and freshwater content. *Journal of Geophysical Research: Oceans*, *128*, e2022JC019247. https://doi.org/10.1029/2022JC019247 (2023).
35. I. V. Polyakov, M. Mayer, S. Tietsche, A. Y. Karpechko, Climate Change Fosters Competing Effects of Dynamics and Thermodynamics in Seasonal Predictability of Arctic Sea Ice. *J. Clim.* **35**, 2849-2865 (2022).
36. J. Morison, R. Kwok, C. Peralta-Ferriz, M. Alkire, I. Rigor, R. Andersen, M. Steele, Changing Arctic Ocean freshwater pathways. *Nature* **481**, 66-70 (2012).
37. M. B. Alkire, J. Morison, R. Andersen, Variability in the meteoric water, sea-ice melt, and Pacific water contributions to the central Arctic Ocean, 2000–2014. *J. Geophys. Res.* **120**, 1573-1598 (2015).
38. I. V. Polyakov, T. P. Rippeth, I. Fer, T. M. Baumann, E. C. Carmack, V. V. Ivanov, M. Janout, L. Padman, A. V. Pnyushkov, R. Rember, Intensification of Near-Surface Currents and Shear in the Eastern Arctic Ocean. *Geophys. Res. Lett.* **47**, e2020GL089469 (2020).
39. L. H. Smedsrud, M. Muilwijk, A. Brakstad, E. Madonna, S. K. Lauvset, C. Spensberger, A. Born, T. Eldevik, H. Drange, E. Jeansson, C. Li, A. Olsen, Ø. Skagseth, D. A. Slater,

F. Straneo, K. Våge, M. Årthun, Nordic Seas Heat Loss, Atlantic Inflow, and Arctic Sea Ice Cover Over the Last Century. *Rev. Geophys.* **60**, e2020RG000725 (2022).

40. H. Hátún, A. B. Sandø, H. Drange, B. Hansen, H. Valdimarsson, Influence of the Atlantic Subpolar Gyre on the Thermohaline Circulation. *Science* **309**, 1841-1844 (2005).
41. N. P. Holliday, S. A. Cunningham, C. Johnson, S. F. Gary, C. Griffiths, J. F. Read, T. Sherwin, Multidecadal variability of potential temperature, salinity, and transport in the eastern subpolar North Atlantic. *J. Geophys. Res.* **120**, 5945-5967 (2015).
42. K. A. Orvik, Long-Term Moored Current and Temperature Measurements of the Atlantic Inflow Into the Nordic Seas in the Norwegian Atlantic Current; 1995–2020. *Geophys. Res. Lett.* **49**, e2021GL096427 (2022).
43. B. I. Barton, Y.-D. Lenn, C. Lique, Observed Atlantification of the Barents Sea Causes the Polar Front to Limit the Expansion of Winter Sea Ice. *J. Phys. Oceanogr.* **48**, 1849-1866 (2018).
44. K. A. Mork, Ø. Skagseth, V. Ivshin, V. Ozhigin, S. L. Hughes, H. Valdimarsson, Advective and atmospheric forced changes in heat and fresh water content in the Norwegian Sea, 1951–2010. *Geophys. Res. Lett.* **41**, 6221-6228 (2014).
45. G. W. K. Moore, K. Våge, I. A. Renfrew, R. S. Pickart, Sea-ice retreat suggests re-organization of water mass transformation in the Nordic and Barents Seas. *Nat. Commun.* **13**, 67 (2022).
46. Ø. Skagseth, T. Eldevik, M. Årthun, H. Asbjørnsen, V. S. Lien, L. H. Smedsrud, Reduced efficiency of the Barents Sea cooling machine. *Nat. Clim. Change.* **10**, 661-666 (2020).
47. J. A. Francis, B. Wu, Why has no new record-minimum Arctic sea-ice extent occurred since September 2012? *Environ. Res. Lett.* **15**, 114034 (2020).
48. J. M. Jackson, W. J. Williams, E. C. Carmack, Winter sea-ice melt in the Canada Basin, Arctic Ocean. *Geophys. Res. Lett.* **39**, L03603 (2012).
49. J. Zhang, Recent slowdown in the decline of Arctic sea ice volume under increasingly warm atmospheric and oceanic conditions. *Geophysical Research Letters*, *48*, e2021GL094780. https://doi.org/10.1029/2021GL094780 (2021).
50. U. S. Bhatt, D. A. Walker, M. K. Raynolds, J. C. Comiso, H. E. Epstein, G. Jia, R. Gens, J. E. Pinzon, C. J. Tucker, C. E. Tweedie, P. J. Webber, Circumpolar Arctic Tundra Vegetation Change Is Linked to Sea Ice Decline. *Earth Interactions* **14**, 1-20 (2010).

51. B. A. Bluhm, M. A. Janout, S. L. Danielson, I. Ellingsen, M. Gavrilo, J. M. Grebmeier, R. R. Hopcroft, K. B. Iken, R. B. Ingvaldsen, L. L. Jørgensen, K. N. Kosobokova, R. Kwok, I. V. Polyakov, P. E. Renaud, E. C. Carmack, The Pan-Arctic Continental Slope: Sharp Gradients of Physical Processes Affect Pelagic and Benthic Ecosystems. *Front. Mar. Sci.* **7**, (2020).
52. P. Snoeijs-Leijonmalm, H. Flores, S. Sakinan, N. Hildebrandt, A. Svenson, G. Castellani, K. Vane, F. C. Mark, C. Heuzé, S. Tippenhauer, B. Niehoff, J. S. Hjelm, J.H., F. J. Schaafsma, R. Engelmann, Unexpected fish and squid in the central Arctic deep scattering layer. *Sci. Adv.* **8**, eabj7536 (2022).
53. R. B. Ingvaldsen, E. Eriksen, H. Gjøsæter, A. Engås, B. K. Schuppe, K. M. Assmann, H. Cannaby, P. Dalpadado, B. A. Bluhm, Under-ice observations by trawls and multi-frequency acoustics in the Central Arctic Ocean reveals abundance and composition of pelagic fauna. *Sci.Rep.* **13**, 1000 (2023).

References from Supplement

54. H. Hersbach, B. Bell, P. Berrisford, S. Hirahara, A. Horányi, J. Muñoz-Sabater, J. Nicolas, C. Peubey, R. Radu, D. Schepers, A. Simmons, C. Soci, S. Abdalla, X. Abellan, G. Balsamo, P. Bechtold, G. Biavati, J. Bidlot, M. Bonavita, G. De Chiara, P. Dahlgren, D. Dee, M. Diamantakis, R. Dragani, J. Flemming, R. Forbes, M. Fuentes, A. Geer, L. Haimberger, S. Healy, R. J. Hogan, E. Hólm, M. Janisková, S. Keeley, P. Laloyaux, P. Lopez, C. Lupu, G. Radnoti, P. de Rosnay, I. Rozum, F. Vamborg, S. Villaume, J.-N. Thépaut, The ERA5 global reanalysis. *Q J R Meteorol Soc.* **146**, 1999-2049 (2020).
55. R. V. Bekryaev, I. V. Polyakov, V. A. Alexeev, Role of Polar Amplification in Long-Term Surface Air Temperature Variations and Modern Arctic Warming. *J. Clim.* **23**, 3888-3906 (2010).
56. H. Zuo, M. A. Balmaseda, S. Tietsche, K. Mogensen, M. Mayer, The ECMWF operational ensemble reanalysis–analysis system for ocean and sea ice: a description of the system and assessment. *Ocean Sci.* **15**, 779-808 (2019).
57. D. P. Dee, S. M. Uppala, A. J. Simmons, P. Berrisford, P. Poli, S. Kobayashi, U. Andrae, M. A. Balmaseda, G. Balsamo, P. Bauer, P. Bechtold, A. C. M. Beljaars, L. van de Berg, J. Bidlot, N. Bormann, C. Delsol, R. Dragani, M. Fuentes, A. J. Geer, L. Haimberger, S. B. Healy, H. Hersbach, E. V. Hólm, L. Isaksen, P. Kållberg, M. Köhler, M. Matricardi, A. P. McNally, B. M. Monge-Sanz, J.-J. Morcrette, B.-K. Park, C. Peubey, P. de Rosnay,

C. Tavolato, J.-N. Thépaut, F. Vitart, The ERA-Interim reanalysis: configuration and performance of the data assimilation system. *Q J R Meteorol Soc.* **137**, 553-597 (2011).

58. T. M. Baumann, I. V. Polyakov, A. V. Pnyushkov, R. Rember, V. V. Ivanov, M. B. Alkire, I. Goszczko, E. C. Carmack, On the Seasonal Cycles Observed at the Continental Slope of the Eastern Eurasian Basin of the Arctic Ocean. *J. Phys. Oceanogr.* **48**, 1451-1470 (2018).
59. R. B. Ingvaldsen, L. Asplin, H. Loeng, The seasonal cycle in the Atlantic transport to the Barents Sea during the years 1997–2001. *Cont. Shelf Res.* **24**, 1015-1032 (2004).
60. W.-J. von Appen, Beszczynska-Möller, A., Schauer, U., Fahrbach, E., Physical oceanography and current meter data from moorings F1-F14 and F15/F16 in the Fram Strait, 1997-2016. https://doi.org/10.1594/PANGAEA.900883. (2019).
61. C. González-Pola, P. Fratantoni, K. M. H. Larsen, N. P. Holliday, S. Dye, K. A. Mork, A. Beszczynska-Möller, H. Valdimarsson, A. Trofimov, H. Parner, H. Klein, B. Cisewski, A. Fontán, K. Lyons, N. Kolodziejczyk, R. Graña, J. Linders, T. Wodzinowski, I. Goszczko, C. Cusack, The ICES Working Group on Oceanic Hydrography: A Bridge From In-situ Sampling to the Remote Autonomous Observation Era. *Front. Mar. Sci.* **6**, (2019).
62. A. Beszczynska-Möller, E. Fahrbach, U. Schauer, E. Hansen, Variability in Atlantic water temperature and transport at the entrance to the Arctic Ocean, 1997–2010. *ICES J. Mar. Sci.* **69**, 852-863 (2012).
63. R. Ingvaldsen, Loeng, H., Ottersen, G., Ådlandsvik, B., Climate variability in the Barents Sea during the 20th century with focus on the 1990s. *ICES Marine Science Symposia* **219**, 160-168 (2003).
64. K. A. Mork, J. Blindheim, Heat loss of the Norwegian Atlantic Current toward the Arctic. *ICES Marine Science Symposia* **219**, 144-149 (2003).
65. V. S. Lien, A. G. Trofimov, Formation of Barents Sea Branch Water in the north-eastern Barents Sea. *Polar Res.* **32**, 18905 (2013).
66. K. Michalsen, P. Dalpadado, E. Eriksen, H. Gjosaeter, R. B. Ingvaldsen, E. Johannesen, L. L. Jorgensen, T. Knutsen, D. Prozorkevich, M. Skern-Mauritzen, Marine living resources of the Barents Sea - Ecosystem understanding and monitoring in a climate change perspective. *Mar. Biol. Res.* **9**, 932-947 (2013).
67. L. A. Codispoti, University of Maryland; Center for Environmental Science; Horn Point Laboratory. Product database composed of physical and nutrient profile data collected in

the Arctic Ocean and adjacent seas from 1928 to 2008 (NODC Accession 0072133). Version 1.1. National Oceanographic Data Center, NOAA. Dataset. (2011).

68. M. Alkire, R. Rember, Geochemical observations of seawater in the eastern Eurasian Basin, Arctic Ocean, 2018. *Arctic Data Center.* doi:10.18739/A2FX73Z1F. (2019).
69. C. Torrence, G. P. Compo, A Practical Guide to Wavelet Analysis. *Bull. Am. Meteorol. Soc.* **79**, 61-78 (1998).
70. I. V. Polyakov, A. V. Pnyushkov, E. C. Carmack, Stability of the arctic halocline: a new indicator of arctic climate change. *Environ. Res. Lett.* **13**, 125008 (2018).
71. M.-L. Timmermans, J. Toole, A. Proshutinsky, R. Krishfield, A. Plueddemann, Eddies in the Canada Basin, Arctic Ocean, Observed from Ice-Tethered Profilers. *J. Phys. Oceanogr.* **38**, 133-145 (2008).
72. A. V. Pnyushkov, I. V. Polyakov, G. V. Alekseev, I. M. Ashik, T. M. Baumann, E. C. Carmack, V. V. Ivanov, R. Rember, A Steady Regime of Volume and Heat Transports in the Eastern Arctic Ocean in the Early 21st Century. *Front. Mar. Sci.* **8**, (2021).
73. A. L. Karsakov, A. Trofimov, V. A. Ivshin, M. Y. Antsiferov, D. V. Gustoev, A. S. Averkiev, Restoration of data on water temperature in the Kola Section for 2016–2017. *Trudy VNIRO 2018* **173**, 193-206 (2016).

Acknowledgments: This study was supported by NSF grant #1724523 (AP, IP), ONR grant # N00014-21-1-2577 (IP). JF was supported by funding from the Woodwell Climate Research Center. Support for RBI was provided by the Research Council of Norway through the Nansen Legacy project (276730) and Institute of Marine Research, Norway. USB was supported by NASA's Arctic Boreal Vulnerability Experiment initiative under grant 80NSSC22K1257. ØS received support from the RCN grant # 295962 NorEMSO.

Author Contributions. All authors participated in data processing and preliminary analysis; AP and IP carried out statistical analysis of reanalysis and mooring data from the eastern Eurasian Basin, RK provided sea ice analysis and processing, MJ provided help interpreting Fram Strait data and formulating objective of the study, JF supervised processing and analysis of atmospheric data, ØS and RBI provided processing and analysis of data from the Nordic and Barents seas, UB added multidisciplinary data and discussion. All authors contributed to interpreting the data and writing the paper.

Author Information. The authors declare no competing financial interests. Correspondence and requests should be addressed to IP (ivpolyakov@alaska.edu).

Data and materials availability: All data used in the analysis are available as described in Supplementary materials.

Supplementary Materials

This PDF file includes:

Materials and Methods

Figs. S1 to S15

References (*54–73*)

Figures

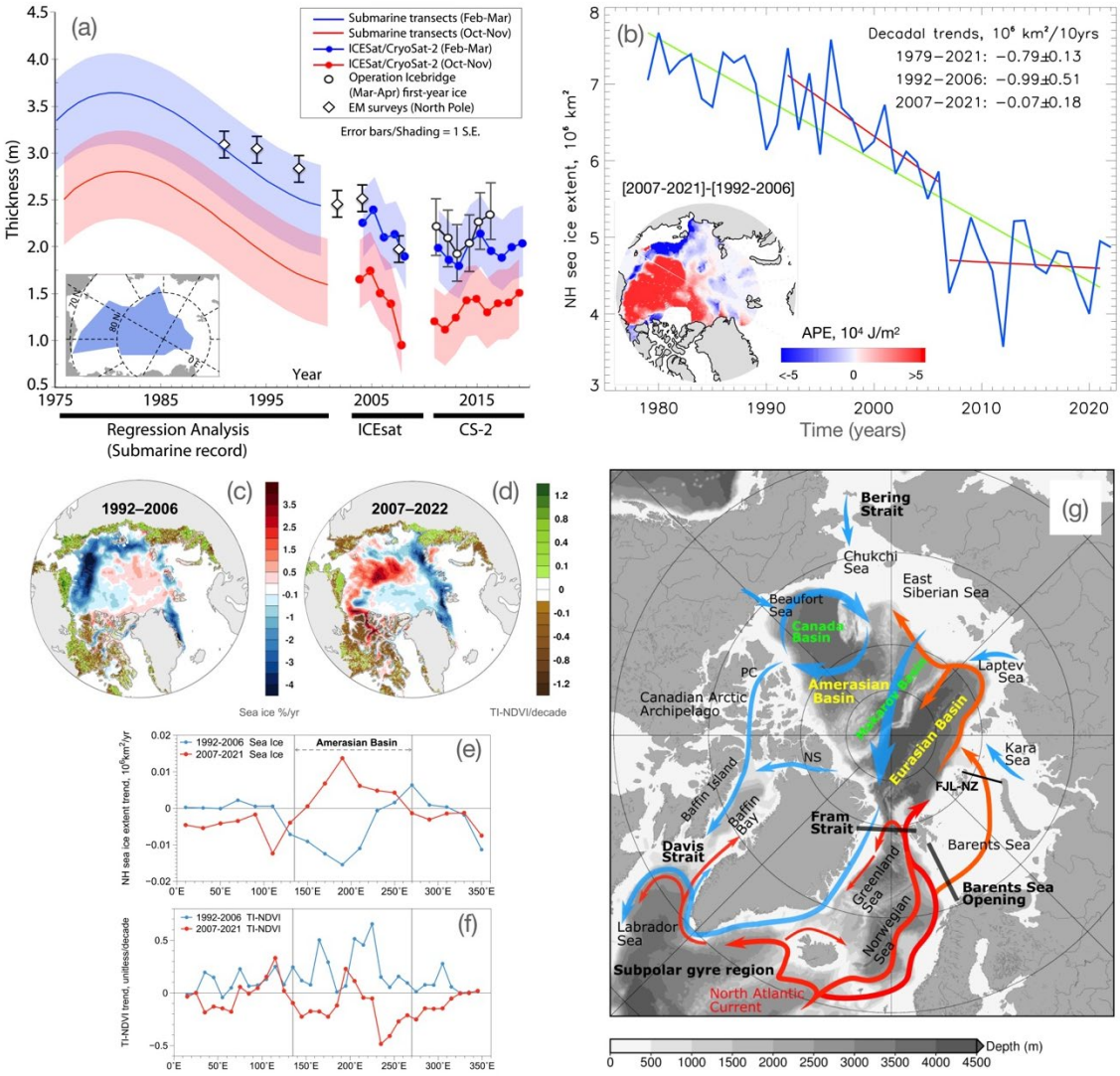

Figure 1: Loss of Arctic sea-ice thickness and extent.

(a) Arctic sea ice thickness changes for autumn (red/dotted red) and winter (blue/dotted blue). Shadings (blue and red) show 1 S.E. ranges from the regression analysis of submarine ice thickness and expected uncertainties in satellite ice thickness estimates. Data release area of submarine data ice thickness data is shown in inset. Satellite ice thickness estimates are for the Arctic south of 88°N. Thickness estimates from more localized airborne/ground electromagnetic surveys near the North Pole (diamonds) and from Operation IceBridge (circles) are shown within the context of the larger scale changes in the submarine and satellite records (*14*).

(b) September sea-ice extent (blue line), the long-term trend (green line), and different regimes of sea-ice extent change in 1992–2006 and 2007–2021 (red segments); the insert shows available potential energy (APE) anomalies in the upper ocean (surface mixed layer

and halocline) for 2007–2017 relative to 1992–2006 (increasing APE signifies stronger stratification suppressing mixing).
(c,d) Maps of trends for (c) the sea-ice concentration (% per year, c) and (d) the summer bi-weekly (time-integrated) Normalized Difference Vegetation Index (TI-NDVI, $decade^{-1}$) over Arctic tundra for 1992–2006 and 2007–2021. The NDVI is a remotely sensed proxy for vegetation productivity and is derived from remotely sensed products in the Arctic. A positive NDVI trend means that the vegetation has more biomass and more photosynthetic productivity; this process is called greening. A negative NDVI trend means that the vegetation has less biomass and is less healthy, and it is called browning.
In (e,f), September sea-ice extent trends (e) and the TI-NDVI (f) for 1992–2006 (blue) and 2007–2021 (red) as a function of longitude.
(g) Diagram of sea ice drift and upper ocean circulation (blue arrows), as well as Atlantic Water circulation (red arrows) (from *15*). FJL-NZ, TPD, and BG indicate Franz Joseph Land – Novaya Zemlya pass, TransPolar Drift, and Beaufort Gyre, respectively.

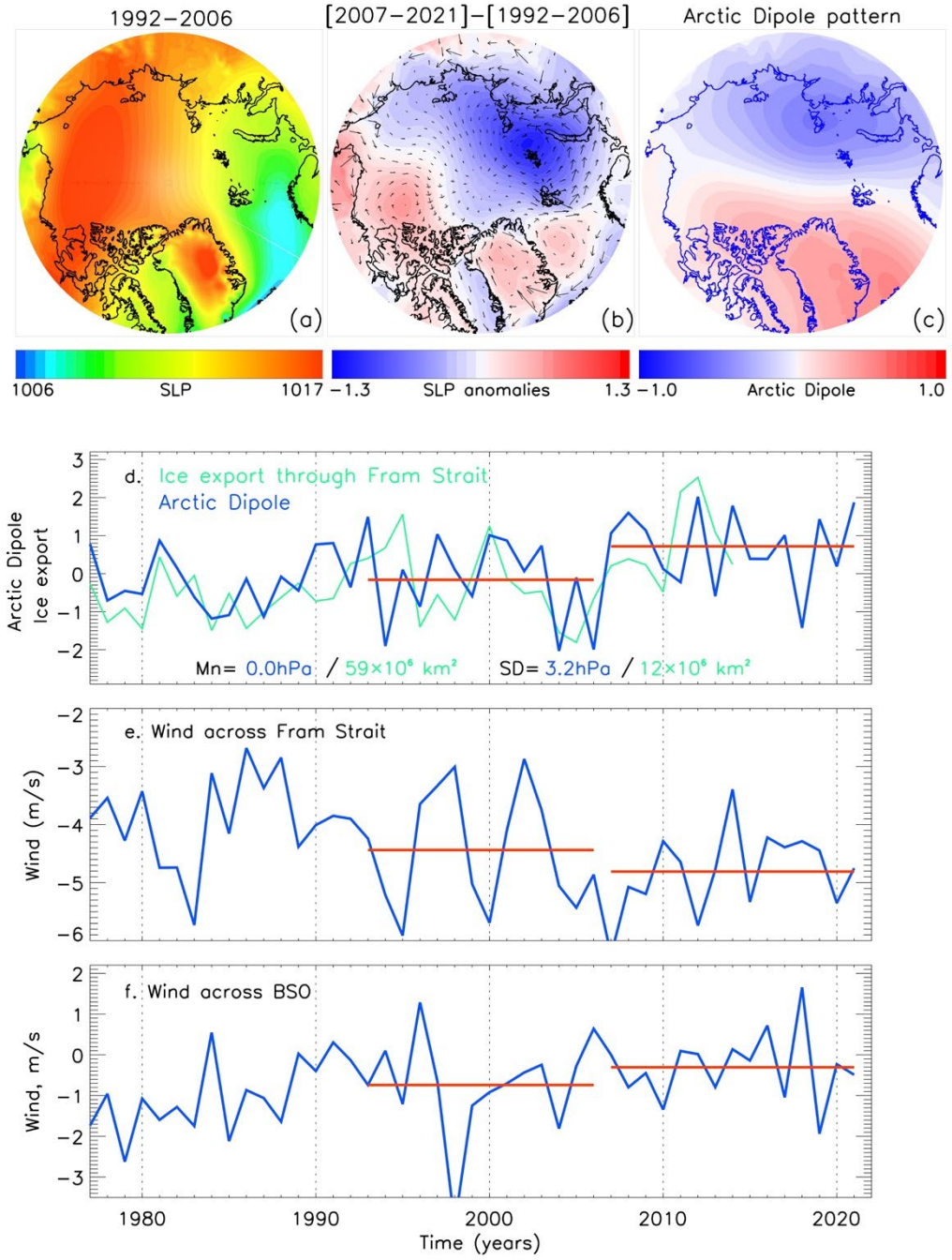

Figure 2: Atmospheric forcing governing the switchgear mechanism. (a) Annual sea level pressure (hPa) averaged over 1992–2006. (b) Annual pressure anomalies (hPa, shading) in 2007–2021 relative to 1992–2006. Vectors show corresponding anomalous geostrophic winds. (c) Arctic Dipole (AD, hPa) pattern, which is correlated with the 2007–2021 pressure anomalies at $R = 0.59$. (d-f) Time series of atmospheric parameters. (d) April-July AD (blue) and March-August ice area transport across Fram Strait (green, from Smedstrud et al. 2017) are reduced to anomalies by subtracting means (Mn) and normalized by standard deviations (SD); AD and ice export are correlated at $R = 0.44$. (e,f) Annual wind across Fram Strait (e) and Barents Sea Opening (f, BSO). In (d-f), red horizontal segments show 1992–2006 and 2007–2021 means.

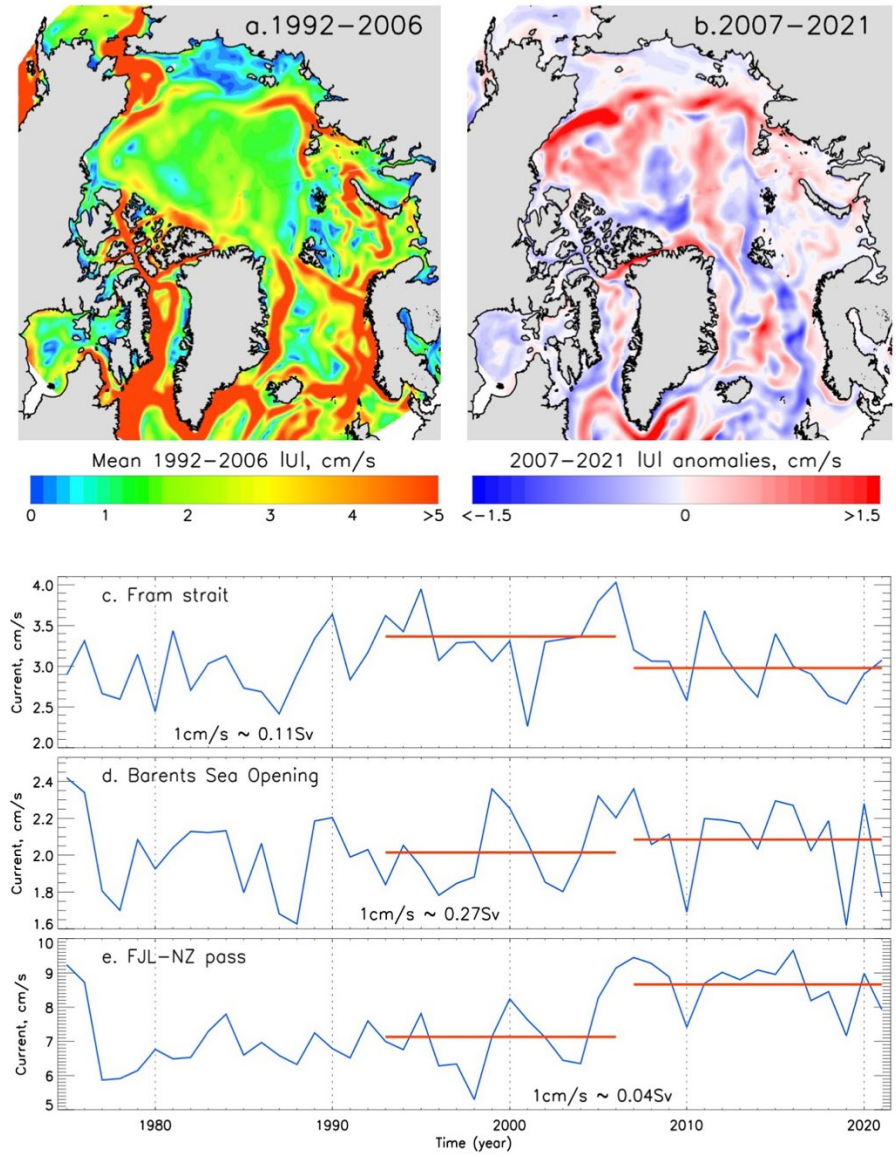

Figure 3: Changes in upper 50 m oceanic circulation from ORAS5 reanalysis between alternate AD phases. (a,b) Maps of (a) 1992–2006 annual mean current speed |U| and (b) 2007–2021 |U| anomalies (relative to the 1992–2006 mean) of the Arctic Ocean and Nordic Seas region with removed low-frequency (1/30yrs cutting off frequency) components using running mean filtering. (c-e) Time series of the ocean annual mean currents inflowing into the Arctic through Fram Strait (c, 80°N, 14°W-10°E), the Barents Sea Opening (d, 71–77°N, 20°E), and the Franz Joseph Land–Novaya Zemlya (FJL–NZ) passage (e, 76.7–80.6°N, 60.5–64.3°E). Red horizontal lines show means over 1992-2006 and 2007-2021. Transfer coefficients from current in cm/s to water transport in Sv (1Sv=10^6 m^3/s) are given in each time series panel. Note the reduced (enhanced) inflow through Fram Strait and enhanced (reduced) Barents Sea throughflow in the years 2007–2021 (1992–2006).

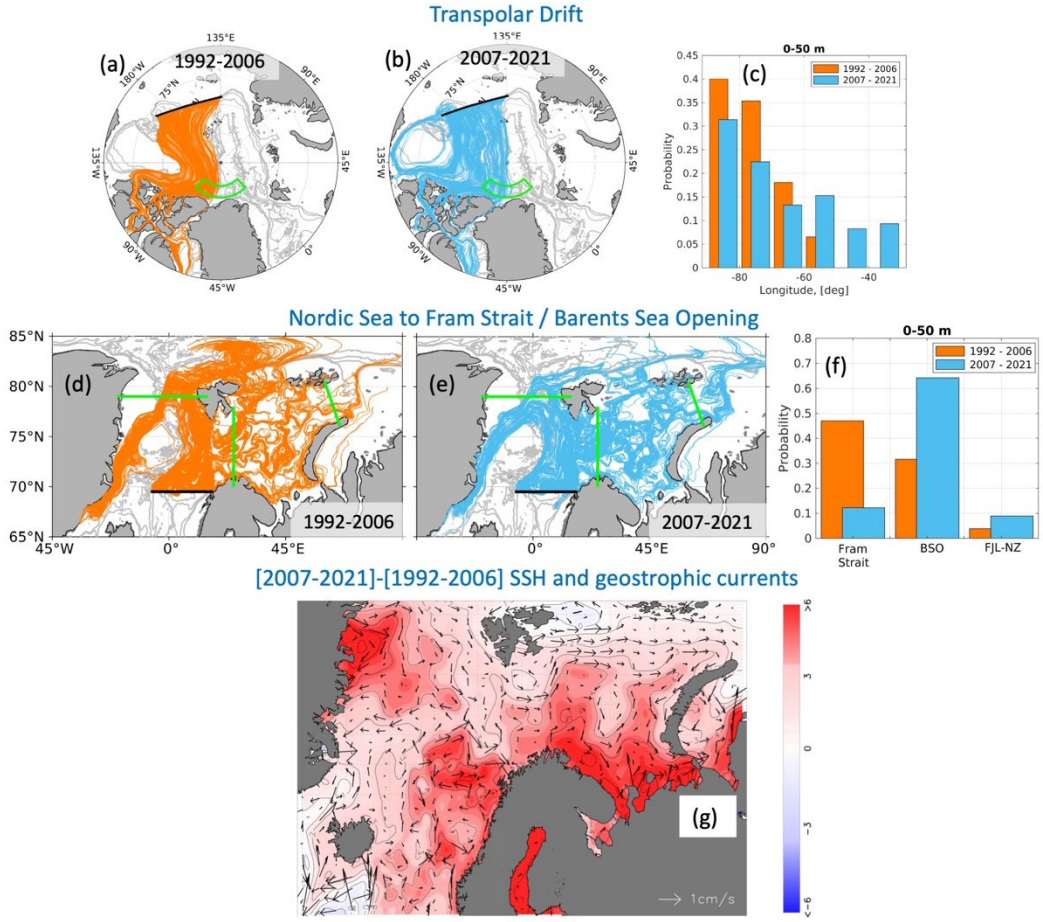

606

607 **Figure 4: Difference of the oceanic circulation patterns between alternate AD phases.** A
608 shift in the Transpolar Drift (a-c), inflows of Atlantic Water from the Nordic Seas across the
609 Barents Sea Opening and Fram Strait (d-f), and anomalous (2007-2021 minus 1992-2006) sea
610 surface height (SSH) and corresponding geostrophic currents (g). (a-c) ORAS5-based
611 trajectories of parcels exiting the central Siberian shelf in 1992–2006 (a) and 2007–2021 (b),
612 and the probability of finding a parcel within the polygon (indicated by the green line) north
613 of the Canadian Archipelago (c). (d-f) ORAS5-based trajectories of parcels released in the
614 Nordic Seas along the sections indicated by the black line in 1992–2006 (d) and 2007–2021
615 (e), and the probability of finding a parcel traveling across the Barents Sea Opening, Fram
616 Strait, and FJL-NZ (indicated by the green lines in (d) and (e)). (g) Satellite-based anomalous
617 SSH and geostrophic currents showing switchgear from Fram Strait to Barents Sea Opening
618 inflow after 2007.

619

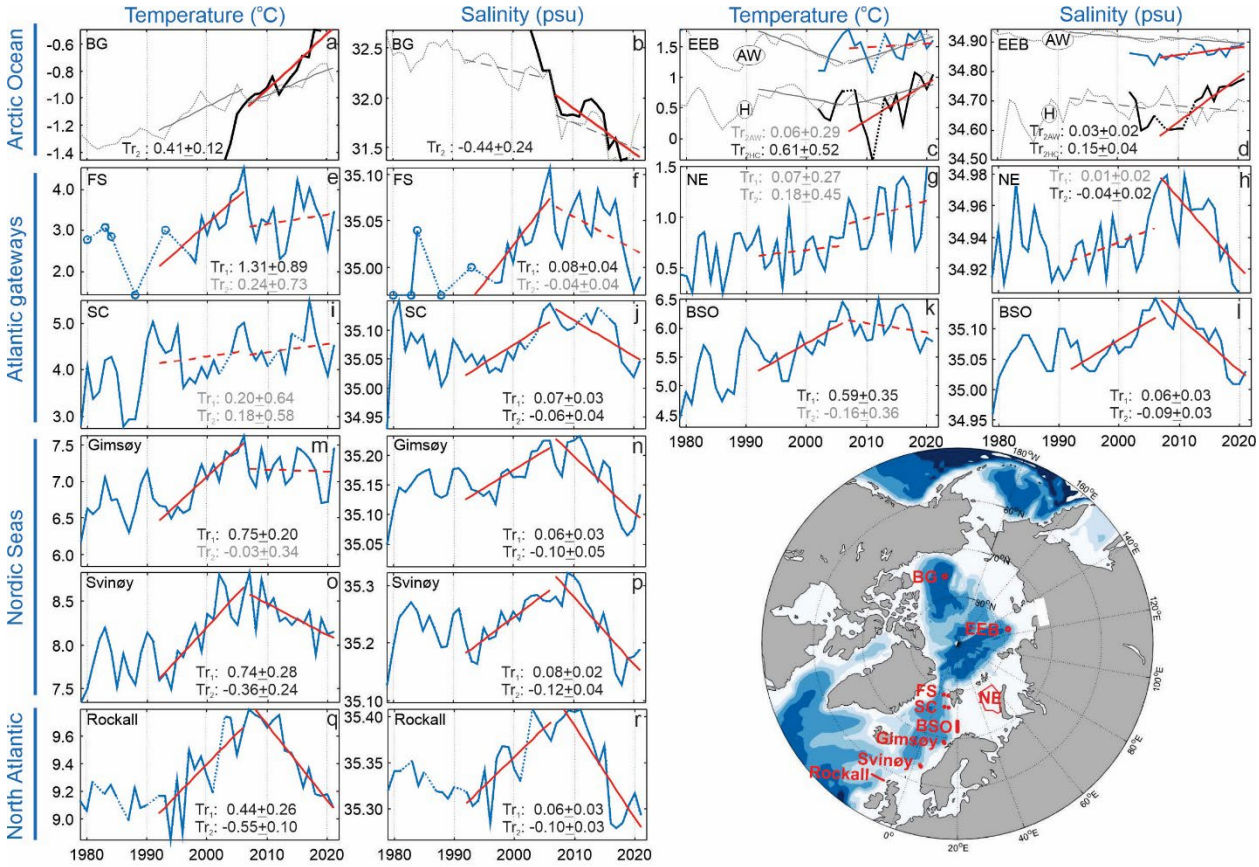

Figure 5: **Contrasting trends of ocean temperature and salinity in the region spanning from the northern North Atlantic to the Arctic Ocean during the positive (2007–2021) and negative (1992–2006) phases of the AD.** Annual time series of water temperature and salinity from repeated observations from the Atlantic Water layer (for depth ranges, see Supplement; blue lines) and halocline (150 m, black lines) (see details in Methods). Observations with substantial gaps were complemented by ORAS5 reanalysis time series (gray lines; note that for the eastern Eurasian Basin (EEB), we plotted ORAS5 temperature, adding 1°C). 95% statistically significant trends are shown by solid red lines and black font; otherwise, dashed red lines and grey font are used. Locations are indicated on the map.